The Atmospheric Circulation and Sea Surface Temperature in the North Atlantic Area in Winter: Their Interaction and Relevance for Iberian Precipitation

EDUARDO ZORITA, VIACHESLAV KHARIN, AND HANS VON STORCH

Max-Planck-Institut für Meteorologie, Hamburg, Federal Republic of Germany

(Manuscript received 19 September 1990, in final form 17 December 1991)

ABSTRACT

The ocean surface–atmosphere relationships in the North Atlantic area in northern winter are empirically examined by canonical correlation analysis (CCA). This analysis is performed from two different points of view. First, the connection between atmospheric circulation anomalies, in terms of monthly mean sea level pressure (SLP) and monthly standard deviation of SLP (σ_{SLP}), and sea surface temperature (SST) anomalies of the Atlantic Ocean are directly examined. Second, the air–sea relationships are indirectly studied through their influence upon precipitation in an area likely to be influenced by the North Atlantic, the Iberian Peninsula.

The canonical correlation analysis yields two pairs of patterns that describe the coherent variations of the combined SST–SLP fields; one pair of patterns for the SST–σ_{SLP} fields and one pair of patterns for the SLP–σ_{SLP} fields. All patterns are dominant in describing variance. A lag cross-correlation analysis of the time coefficients indicates that monthly mean SLP varies simultaneously with σ_{SLP} but is leading monthly mean SST slightly. These results are consistent with the hypothesis that anomalies of the atmospheric circulation are mainly responsible for the appearance of anomalous wintertime SST and with the notion that the intramonthly variability of the atmosphere (σ_{SLP}) is coupled to the mean flow (SLP).

With respect to Iberian precipitation, one well-defined CCA pair of patterns of regional rainfall and, respectively, SLP and SST is found. Above-normal Iberian precipitation is connected with a "high-index" North Atlantic SLP distribution and below-normal SST in most of the Atlantic north of 20°N. The dominant process responsible for the variability of rainfall appears to be the intensity of the westerly wind and the frequency of storms imbedded in it, not the presence of regional or remote SST anomalies.

It is concluded that a large-scale SLP pattern in the North Atlantic, similar to the first EOF of the SLP field, is instrumental in generating both the Iberian precipitation and Atlantic SST variability on the seasonal time scale.

1. Introduction

a. *Atmosphere–ocean interaction in the North Atlantic area*

It is well known that extratropical sea surface temperature anomalies (SST) and atmospheric circulation anomalies are linked (e.g., Bjerknes 1962; Ratcliffe and Murray 1970; Rogers and van Loon 1979; Palmer and Sun 1985; Dymnikov and Filin 1985a,b). There is, however, no widely accepted answer to the question of whether the anomalous SST forcing on the atmosphere is more efficient than atmospheric forcing of the SST or vice versa.

The notion that anomalous SST is exerting a significant impact on the atmospheric circulation has been supported by numerous experiments with general circulations models (GCMs; e.g., Rowntree 1972; Hannoschöck and Frankignoul 1985; Frankignoul and Molin 1988; Palmer and Sun 1985; Dymnikov and Filin 1985b; Pitcher et al. 1988; Hense et al. 1990; Lau and Nath 1990) and by to some extent inconclusive empirical studies (Namias 1978; Namias and Cayan 1982). However, Barnett et al. (1984) found that extratropical North Atlantic SST has no statistically significant skill in specifying or predicting Eurasian surface air temperature on a yearly time scale. Also, in the Hense et al. (1990) GCM experiment, the response to Atlantic SST anomalies was twofold: a relatively strong upper-level response to tropical SST anomalies and a weak and shallow local response to extratropical SST anomalies.

The opposite view, that at monthly to yearly time scales the extratropical SST is mostly passively reacting to atmospheric circulation anomalies, has been hypothesized by Bjerknes (1962). Davis (1976) found ocean–atmosphere lag correlations to be asymmetric, with the atmosphere leading the ocean. In a GCM study, Luksch et al. (1990) were able to reproduce most of the wintertime SST low-frequency variability in the North Pacific as a response to anomalous atmospheric flow. These results, together with the fact that characteristic spatial scales of SST anomalies compare with the spatial scales of atmospheric anomalies, support

Corresponding author address: Dr. Hans von Storch, Max-Planck-Institut für Meteorologie, Bundestrasse 55, W-2000 Hamburg, Federal Republic of Germany.

the hypothesis that SST anomalies are mainly driven by atmospheric circulation anomalies (e.g., Frankignoul 1985 and references therein).

It has been proposed that SST anomalies govern, at least partly, rainfall anomalies in neighboring continental regions (e.g., Hunt and Gordon 1988 and references therein). Lamb and Peppler (1987), on the other hand, found a close relationship between the North Atlantic Oscillation (NAO) (van Loon and Rogers 1978; Rogers 1984; Barnston and Livezey 1987; Lamb and Peppler 1987; Glowineka-Hense 1990) and the rainfall in northwest Africa and suggested a similar situation for the precipitation over the Iberian Peninsula. They speculated that SST anomalies might be partly responsible for the NAO. The last part of this paper is devoted to the clarification of the relationship between the interannual variabilities of Atlantic SST and SLP and of Iberian rainfall.

b. *Strategy of this study*

The present study is a statistical analysis of the linkage between the ocean and the atmosphere in the North Atlantic area and of Iberian rainfall in the winter season. For this purpose, canonical correlation analysis (CCA) is applied to the monthly means of the sea surface temperature (SST) and sea level pressure (SLP), to the monthly SLP standard deviation (σ_{SLP}), and to station data of Iberian monthly mean rainfall. The former two quantities are intended to represent the low-frequency variability on intermonthly and longer time scales of the atmosphere and the oceanic mixed layer, whereas the SLP standard deviation is related to the intramonthly variability of the atmosphere, associated with synoptic baroclinic activity, as well as with more slowly evolving weather systems over the North Atlantic.

The result of the CCA is a set of pairs of patterns whose coefficient time series correlate optimally. One might envisage how the SST, SLP, σ_{SLP}, and regional rainfall patterns relate to each other and how the respective coefficients exhibit lags, if the SST anomalies are mainly caused by atmospheric anomalies and vice versa.

If it is the SST acting on the atmosphere, the correlations between monthly mean SST and atmospheric parameters should be maximum at lag 0 since the time scale of the atmospheric response to the SST anomalies is of the order of a few days only. With respect to patterns, the following concept is reasonable: a surplus of warm surface water will be connected with an extra flux of latent and sensible heat into the atmosphere. In the framework of simplified theory (Egger 1977; Webster 1981) this anomalous heating in the extratropics is balanced by horizontal advection of temperature ("advective limit"); that is, the low-level atmosphere will be warmer and wetter to the east of the warm SST anomaly. Thus, the surface air pressure will be lower there. The static stability of the atmosphere will be reduced so that, possibly, more storms might develop. To summarize (Fig. 1a): if extratropical SST anomalies do exert a significant effect on the atmosphere, then one might expect to the east of a positive (negative) SST anomaly negative (positive) SLP anomalies and higher (lower) than normal intramonthly variability (σ_{SLP}) to the south (north) of SLP anomaly. We will return to this concept in the final discussion. SST anomalies that are instrumental in causing an excess of rainfall anomalies would be positive and located upstream of the precipitation. The additional reservoir of water vapor would be advected to the Iberian Peninsula where part of it eventually would precipitate. One would expect this extra pool of warm water to be in the eastern part of the central Atlantic.

If the SST anomalies may be understood as mainly being generated by anomalous atmospheric flow, the lag correlation should be maximum when the ocean

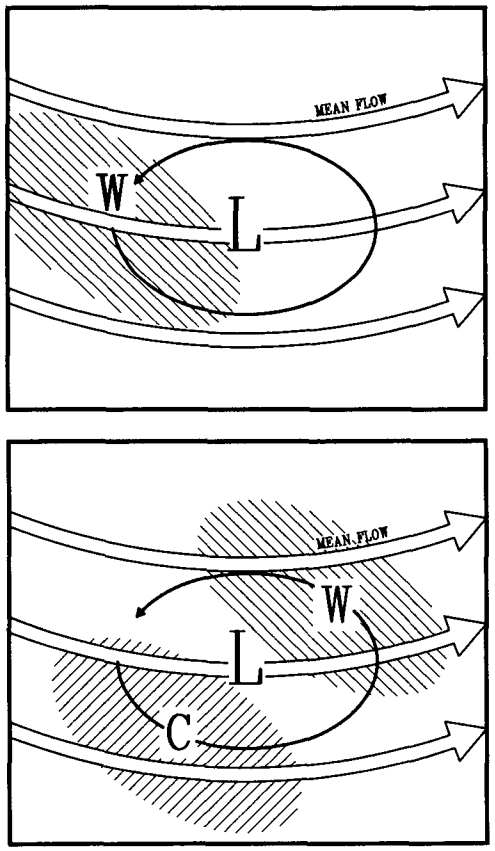

FIG. 1. Schematics of the expected form of (a) an atmospheric response to anomalous extratropical SST [cf. Egger (1977) or the advective limit concept of Webster (1981)] and of (b) the SST response to anomalous atmospheric conditions in the westerly wind belt. Mean westerly flow is represented by big open arrows. Hatched areas represent anomalous warm ("W") or cold ("C") surface water. Anomalous atmospheric cyclonic circulation is denoted by "L" and thin solid arrows.

lags the atmosphere by zero to one month, since the response time of the mixed layer is of the order of a few weeks.

The following ideas, which can be found in Bjerknes' (1962) pioneering work on the establishment of atmospherically induced SST anomaly patterns, are supported by the GCM study of Luksch et al. (1990) and are in accordance with plausibility arguments (e.g., Kalnay et al. 1986) and empirical studies (Cayan 1990). In the presence of a westerly background flow, an anomalous cyclonic flow in the atmosphere will be connected with anomalous cooling at the cyclone's western and southern flank and warming at its eastern and northern flank, due to anomalous latent and sensible heat fluxes. Another process that is of significance for the SST is that the zonal wind stress will be increased at its southern flank and reduced at its northern edge. Thus, one might expect in the ocean a net cooling equatorward and westward of the cyclone and a net heating northward and eastward of it (Fig. 1b). Upwelling due to the anomalous circulation is of secondary importance (Luksch et al. 1990).

Possibly, anomalies of Iberian rainfall are mainly caused by anomalies of the atmospheric circulation; thus, stronger westerly winds in the Iberian region would advect more maritime air, and the area of baroclinicity would be shifted southward so that more synoptic systems would travel to the peninsula.

The oceanic and atmospheric patterns that are derived by the canonical correlation analysis (CCA) will be discussed in terms of the simplified concepts given above. These ideas have been already used in the context of long-range weather forecasting to discriminate situations in which SST anomalies should (or should not) be included in a prediction scheme (Mo et al. 1987). Here they are applied in a climatic time scale.

c. *Organization of the paper*

The paper is organized as follows. Section 2 describes the dataset used. The statistical method, canonical correlation analysis (CCA), is briefly presented in section 3. The results on the relationship between North Atlantic scale SLP, σ_{SLP}, and SST anomalies are given and discussed in section 4. Finally, in section 5, the dependence of Iberian rainfall on anomalous SST and on anomalous atmospheric flow is considered. The results are discussed and summarized in section 6, closing the paper.

2. Data

The data used in this study are time series of monthly means of SLP, SST, and time series of intramonthly standard deviation of SLP (σ_{SLP}) taken from the COADS (Woodruff et al. 1987). Further details about the construction, characteristics, and quality of these time series can be found in Cayan (1990). The original COADS data, with a resolution of 2° × 2°, were averaged onto a 4° latitude × 10° longitude grid to enhance the signal-to-noise ratio. The analysis covers the North Atlantic sector north of about 20°N, and the period of observations includes the winters (December–February) between 1950 and 1986 (for σ_{SLP}, the winter period 1950–79). Some gaps were filled by linear interpolation in time. At each grid point anomalies have been obtained by subtracting the long-term monthly mean from the original values. Prior to the CCA the anomalies at each grid point were weighted by the square root of the latitude cosine to take into account the latitudinal variation of the grid box sizes. However, when presenting the results in the following sections, the area weightings have been removed from the data.

Precipitation records were obtained from the World Meteorological Station Climatology (WMSC) and were kindly supplied by the National Center for Atmospheric Research (NCAR). Twenty-nine stations on the Iberian Peninsula are considered. Their records usually span the period 1951–86. Since monthly mean precipitation values can be biased by small-scale and short-lived weather systems, total seasonal (DJF) anomalies are considered. When considered simultaneously with the precipitation data, the SLP and SST fields were seasonally averaged.

3. Canonical correlation analysis

In this section, a short summary of the concept of the canonical correlation analysis (CCA) is given. A more detailed description of this method can be found in Anderson (1984). This technique was originally developed by Hotelling (1936) and has been in use in atmospheric and oceanic sciences for a few years (e.g., Barnett and Preisendorfer 1987; Metz 1989); a slightly modified technique was used by Dymnikov and Filin (1985a).

Basically, the CCA selects a pair of spatial patterns of two space–time dependent variables such that their time components are optimally correlated. Given two sets of variables, $\mathbf{x} = (x_1, \cdots, x_N)^T$ and $\mathbf{y} = (y_1, \cdots, y_M)^T$, with zero time means ($\langle \mathbf{x} \rangle = \langle \mathbf{y} \rangle = 0$), CCA finds new variables, U_i and V_j, as linear combinations of $\mathbf{x}$ and $\mathbf{y}$, $U_i = \alpha_i^T \mathbf{x}$, and $V_j = \beta_j^T \mathbf{y}$, which give the maximum correlations $\langle U_i V_i \rangle$ under the conditions

$$\begin{aligned} \langle U_i U_k \rangle &= \delta_{ik} \\ \langle V_j V_1 \rangle &= \delta_{j1} \\ \langle U_i V_j \rangle &= \lambda \delta_{ij}, \end{aligned} \tag{1}$$

where angle brackets indicate time averaging. Mathematically, the problem is reduced to the following coupled eigenproblem with the same eigenvalues λ^2:

$$\begin{cases} \mathbf{C}_{xx}^{-1} \mathbf{C}_{xy} \mathbf{C}_{yy}^{-1} \mathbf{C}_{xy}^T \alpha = \lambda^2 \alpha \\ \mathbf{C}_{yy}^{-1} \mathbf{C}_{xy}^T \mathbf{C}_{xx}^{-1} \mathbf{C}_{xy} \beta = \lambda^2 \beta, \end{cases} \tag{2}$$

where $\mathbf{C}_{xx}$ and $\mathbf{C}_{yy}$ are the autocovariance matrices and $\mathbf{C}_{xy}$ is the cross-covariance matrix. It can be shown that the eigenvalue λ_i^2 is just the squared correlation $\langle U_i V_i \rangle^2$. The pair of eigenfunctions α_1 and β_1 associated with the maximum eigenvalue gives the maximum correlation between U_1 and V_1.

To avoid quasidegeneracy of the autocovariance matrices, it is highly advisable to reduce the spatial degrees of freedom, previous to CCA. This can be done, for example, by projecting the original data onto their empirical orthogonal functions (EOFs) and retaining only a limited number of them, explaining most of the total variance. This also serves as a data-filtering procedure to eliminate noise, although it can exclude potentially useful information. The new variables that enter the CCA are, therefore, the EOF time series. Note that in this case, the matrices $\mathbf{C}_{xx}$ and $\mathbf{C}_{yy}$ are diagonal so their inverses can be more easily computed. After obtaining the canonical correlation time series U_i and V_i in terms of linear combinations of the EOF time series, the canonical correlation patterns can be easily calculated in terms of the original variables by means of the relations

$$\mathbf{g}_i = \mathbf{C}_{xx}\alpha_i = \langle U_i \mathbf{x} \rangle$$

and

$$\mathbf{h}_j = \mathbf{C}_{yy}\beta_j = \langle V_j \mathbf{y} \rangle. \quad (3)$$

Thus, the canonical correlation patterns $\mathbf{g}$ and $\mathbf{h}$ represent the local covariance between the considered random field, $\mathbf{x}$ and $\mathbf{y}$, and the scalar expansion coefficients U and V. Since U and V are normalized (1), the patterns $\mathbf{g}$ and $\mathbf{h}$ represent the "typical" strength of the signal.

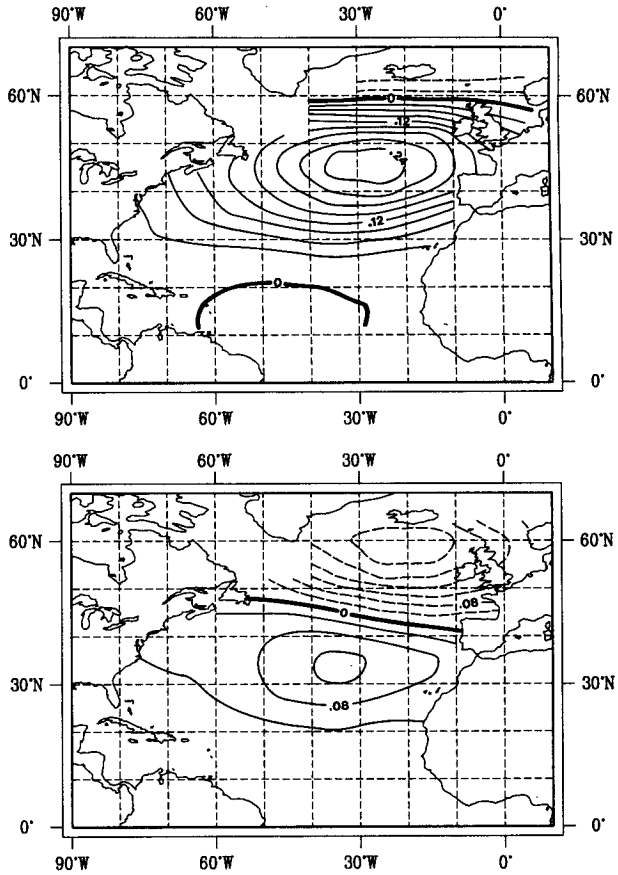

FIG. 2. First (a) and second (b) EOFs of monthly mean sea level pressure (SLP) in the North Atlantic area in the winter (DJF) season. The variances are $(26\ \text{mb})^2$ and $(23\ \text{mb})^2$, explaining 38% and 29% of the total variance. Continuous lines mark positive values, and dashed lines negative values. The zero line is in bold.

4. Relationship of SLP, σ_{SLP}, and SST anomalies in the North Atlantic area

The canonical correlation analysis is applied to the EOF time series. The EOFs of SLP and SST in the Atlantic region have been studied previously (SLP: Kutzbach 1970; Glowienka-Hense 1990; SST: Weare 1977; Wallace et al. 1990) and are presented in section 4a to check the stability of the patterns if derived from a different data source. The EOFs are also examined if they are sensitive to the "varimax rotation" (Richman 1986), which yields "simple spatial patterns." In section 4b, the results of the CCA are given.

a. EOFs of SLP, SST, and σ_{SLP}

The first two EOFs of SLP explain 38% and 29% of the total variance (Fig. 2). Interestingly, the varimax-rotated SLP-patterns are essentially the same as the raw EOFs. This could be expected since the original EOFs already exhibit a fairly simple structure. The spatial structures and the variances are in good agreement with previously published results (Kutzbach 1970; Glowienka-Hense 1990).

The first two EOFs of the sea surface temperature anomalies (Fig. 3) are responsible for 22% and 16% of the total variance. In contrast to the SLP EOFs, these patterns are not of "simple structure," and the varimax rotation leads to significantly different structures (not shown). In the first EOF three relevant but not very large areas are identified: the west Atlantic off Newfoundland and south of Greenland, the upwelling region at the western African coast, and the west Atlantic off the United States coast exhibiting anomalies of opposite sign. The varimax rotation attributes each of the three areas just mentioned to the first three rotated patterns. The structure of the second EOF is of somewhat larger scale with a dividing line roughly at 30°N. The spatial patterns and variance found agree with previous studies (Weare 1977; Wallace et al. 1990).

The first two EOFs of the σ_{SLP} represent 27% and 12% of the total variance (Fig. 4). The first EOF is positive everywhere and is similar to that for SLP. The second EOF explains about 12% of the variance and

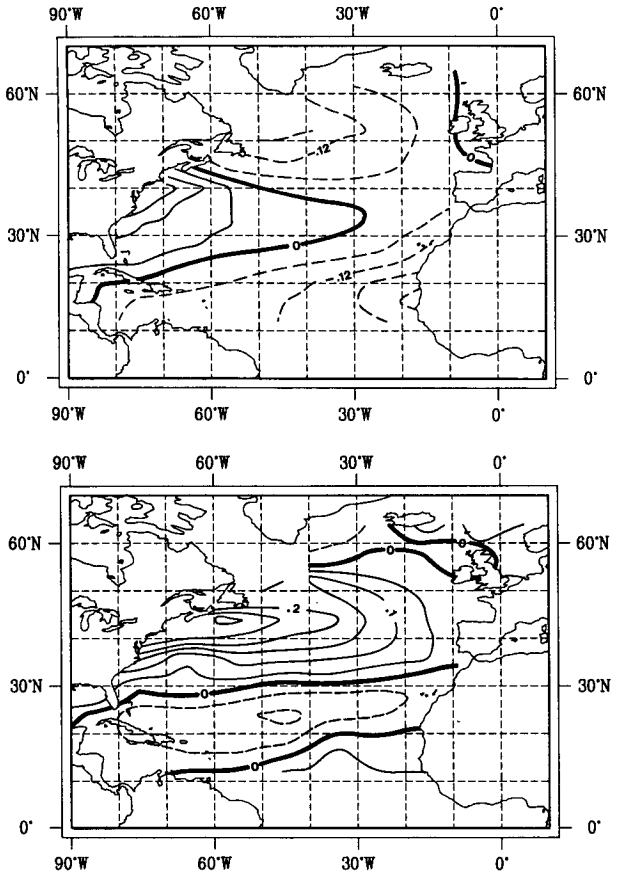

FIG. 3. First (a) and second (b) EOFs of monthly mean sea surface temperature (SST) in the North Atlantic in the winter (DJF) season. The variances are $(2.6\ \mathrm{K})^2$ and $(2.2\ \mathrm{K})^2$, explaining 22% and 16% of the total variance. Continuous lines mark positive values, and dashed lines negative values. The zero line is in bold.

has a dipole structure with one center of action located south of Iceland and the other one farther south at 45°N latitude. A weakly marked maximum also appears near the North American east coast, south of Newfoundland.

Lau (1988) analyzed EOFs of bandpass-filtered (baroclinic time scale) geopotential height variance in winter. Their patterns deviate from ours, indicating that a substantial contribution to the intramonthly variance is made by processes on time scales above the baroclinic scale.

b. Results of the canonical correlation analysis

The first five EOFs of the SLP, SST, and σ_{SLP} fields have been retained for the subsequent CCA. These EOFs explain 87%, 62%, and 62% of the total variance of these three fields, respectively. Since the explained variance for SST (62%) and σ_{SLP} (62%) may seem small, the sensitivity of the canonical correlation results to EOF truncation has been checked. The same CCA calculations were performed using the first 10 or 15 EOFs for SST (77% or 84% explained variance, respectively) and σ_{SLP} (78% or 86% explained variance, respectively), and essentially the same results were obtained. Also, the use of seasonal means (DJF) instead of monthly winter means did not notably change the results.

To gain a deeper insight into the causal relationships among the three fields, the CCA coefficient time series were shifted relative to each other by ±1 month, and the lagged correlations were calculated (Table 1). Approximately the same correlations and patterns were found when the CCA was made for the input vector time series shifted relative to each other.

1) SLP–SST

The first SLP–SST pair of patterns have a maximum correlation of .56 and explain 21% of the SLP variance and 19% of the SST variance (Fig. 5). The two patterns are consistent with the hypothesis of atmospheric anomalies causing SST anomalies (see the Introduc-

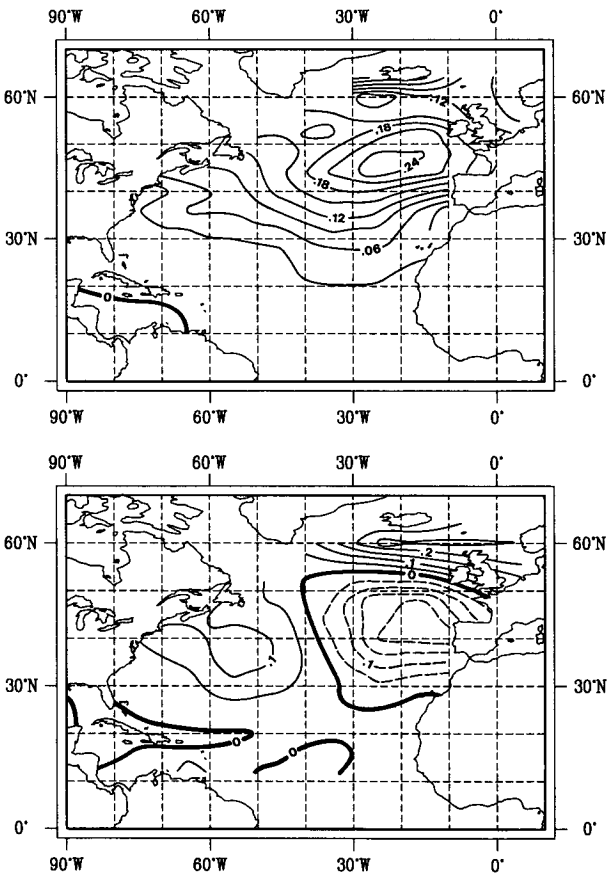

FIG. 4. First (a) and second (b) EOFs of the monthly mean SLP standard deviation σ_{SLP} in the North Atlantic area in the winter (DJF) season. The variances are $(9.3\ \mathrm{mb})^2$ and $(6.1\ \mathrm{mb})^2$, explaining 27% and 12% of the total variance. Continuous lines mark positive values, and dashed lines negative values. The zero line is in bold.

TABLE 1. Lagged correlation coefficients of the CCA time series. A lag of −1 indicates that the first field leads the second one by one month.

	SLP–SST			SLP–σ_{SLP}			SST–σ_{SLP}		
CCA pair	−1	0	+1	−1	0	+1	−1	0	+1
First	.65	.56	.09	.02	.52	.14	.25	.52	.62
Second	.48	.47	.03	−.06	.45	.20	.46	.49	.56

tion). The main features of the SLP pattern are an increase of the westerly wind at about 50°N and an anomalous anticyclonic circulation centered at 30°N, 40°W. North of the anticyclone, where the westerly wind is enhanced, the ocean surface is cooler than normal. West of the anticyclone, where the southerly winds are enhanced, the ocean is warmed substantially. The SST anomalies off the African coast may be understood as a local response to anomalous winds: coastal upwelling is increased if stronger than normal northerly winds are present. In the case of a circulation with reduced westerlies at about 50°N and an anomalous cyclonic flow in the southern part of the area considered, opposite SST anomalies prevail. The CCA coefficient time series support the leading role of the atmosphere: the 1-month lag correlation is .65 if SLP leads the SST but only .09 if SLP is lagging (Table 1).

The second CCA pair goes with a correlation of .47 (Fig. 6). The SLP pattern explains 31% of the total SLP variance, and the SST pattern explains 15%. This second CCA pair can be explained in the same manner as the first one. If SLP leads SST by 1 month, the lag correlation is .48 compared to .03 if SLP lags by 1 month (Table 1).

The first pair's SST pattern (Fig. 5b) resembles the first EOF of SST (Fig. 3a), and the second CCA pair's SST pattern (Fig. 6b) is similar to the second SST EOF (Fig. 3b). With respect to SLP, the order is reversed; however, the second CCA pair's SLP pattern (Fig. 6a)

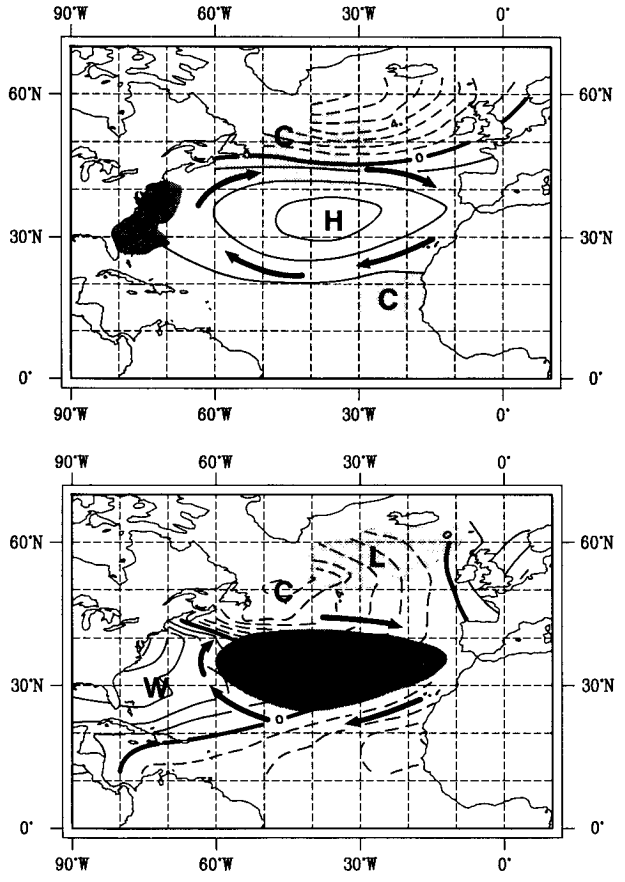

FIG. 5. The patterns of the first canonical pair of SLP (mb; countour interval 1 mb) and SST (K; contour interval 0.1 K) in the North Atlantic area. The correlation between the corresponding time components is 0.56. They explain 21% and 19% of the total variance. In each figure, hatched areas correspond to maxima or minima in the other figure. Continuous lines mark positive values, and dashed lines negative values. The zero line is in bold.

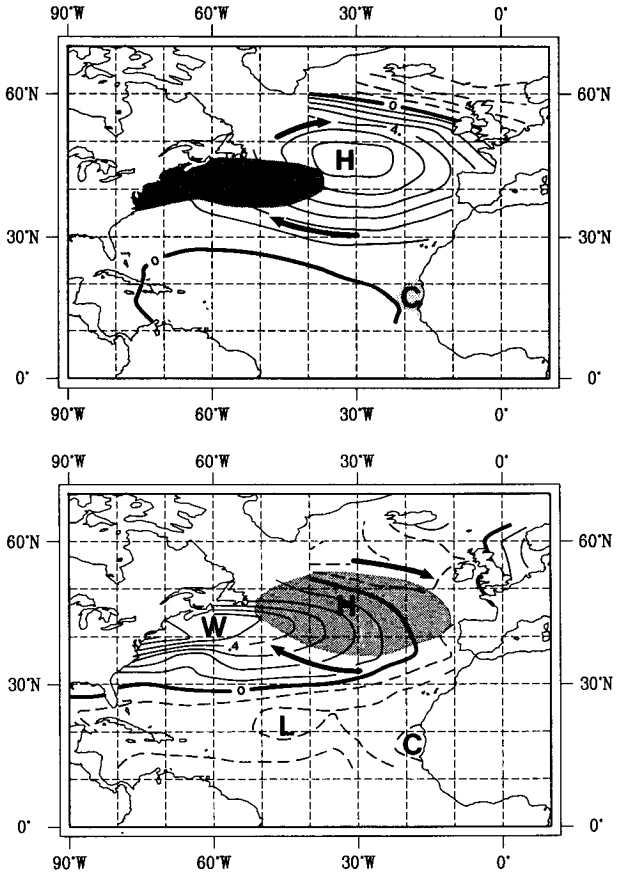

FIG. 6. The patterns of the second canonical pair of SLP (mb; contour interval 1 mb) and SST (K; contour interval 0.1 K) in the North Atlantic area. The correlation between the corresponding time components is 0.47. They explain 31% and 15% of the total variance. In each figure, hatched areas correspond to maxima or minima in the other figure. Continuous lines mark positive values, and dashed lines negative values. The zero line is in bold.

is similar to the first SLP EOF (Fig. 2a) and represents most of the month-to-month variance (31%). The first pair's SLP (Fig. 5a) is like the second EOF (Fig. 2b) and represents only 21% of the SLP variance. Seemingly, the SST response to the first SLP EOF is weaker than the response to the second EOF, which describes the variations of the outflow of cold air from the American continent.

The SLP EOFs exhibit "simple structures" that are almost unaffected by the varimax rotation. In contrast, the SST EOFs have structured "nonsimple" patterns (Fig. 3). Interestingly, the CCA reveals that these "simple" atmospheric patterns and "nonsimple" oceanic patterns are causally linked to each other. That is, the most energetic SST EOFs are not representative of the ocean's dynamics but instead reflect the ocean's response to the coherent atmospheric forcing. Thus, in this case, the use of rotating procedures to identify simple structures among the leading EOFs is misleading, and the original, unrotated, EOFs with a more complicated spatial structure are more satisfactory in describing the system's physics.

2) SLP–σ_{SLP}

The correlation of the first CCA pair of SLP and σ_{SLP} is .52 (Fig. 7). Both the SLP and σ_{SLP} patterns explain a large portion of variance (36% and 24%) and have similar structures but with opposite signs. The lag correlations indicate that the anomalies of the monthly mean and of the monthly standard deviation occur together: The ±1-month lag correlations between SLP and σ_{SLP} are negligible (.02 and .14) compared to the simultaneous correlation of .52. Thus, positive (negative) SLP anomalies are associated with reduced (enhanced) intramonthly variability of the atmosphere in this region. This correspondence between intramonthly and intermonthly variability of SLP agrees with previous results obtained by Cayan (1990).

The second canonical correlation coefficient is .45. The corresponding canonical patterns (not shown) have a dipole structure and also show spatial coincidence of intermonthly and intramonthly variability.

3) SST–σ_{SLP}

The SST and σ_{SLP} patterns (Fig. 8) of the first CCA pair (correlation .52) of these two parameters explain somewhat less variance than in the other two combinations, namely only 12% and 14%. The extremes in the two patterns are well separated. In the SST field, the minimum is off the United States coast, whereas the maximum of the intramonthly SLP variance is near Iceland. The SST pattern resembles the SST pattern obtained in the SST–SLP analysis (Fig. 6b), although with opposite sign.

The patterns of the SST–σ_{SLP} CCA are not consistent with the idea that ocean surface temperatures might

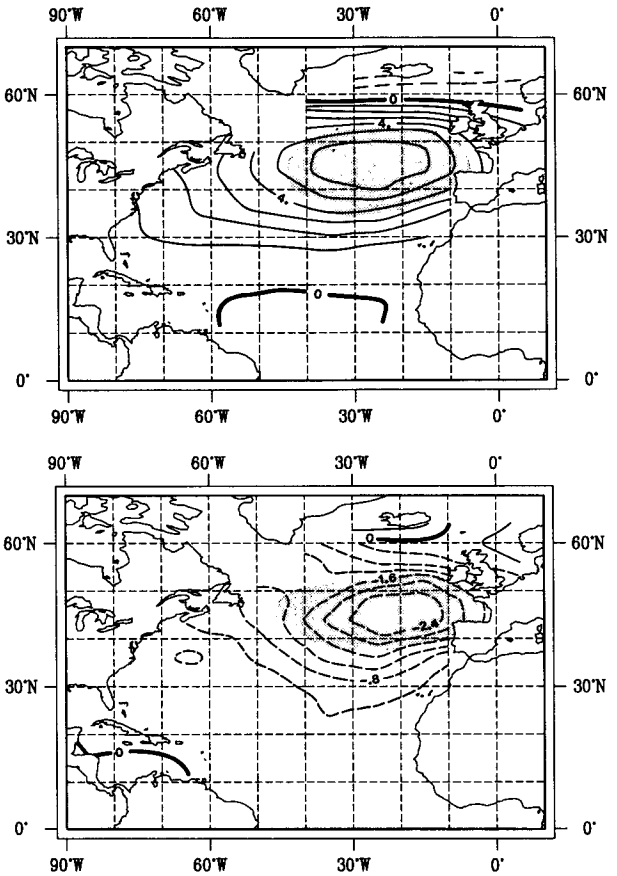

FIG. 7. The patterns of the first canonical pair of SLP (mb; contour interval 1 mb) and σ_{SLP} (mb; contour interval 0.4 mb) in the North Atlantic area. The correlation between the corresponding time components is 0.52. They explain 36% and 24% of the total variance. In each figure, hatched areas correspond to maxima or minima in the other figure. Continuous lines mark positive values, and dashed lines negative values. The zero line is in bold.

enhance the atmospheric variability (see the Introduction). In particular, the SST upstream of the region of increased intramonthly atmospheric variability is not warmer than normal but colder. Also, the 1-month lag correlations between SST and σ_{SLP} are asymmetric: If the σ_{SLP} leads (lags) SST by 1 month, the correlation is .62 (.25) (Table 1).

The patterns, and the lag correlations, are consistent with the negative SST anomalies being forced by more storms traveling along the North Atlantic belt between 40° and 60°N. The increased wind stress on their southern flanks will be connected with extra mixing (thus cooling), and the cold-air outbreaks off the American coast will be associated with strong anomalous upward heat fluxes.

5. Precipitation over the Iberian Peninsula

We first present in section 5a the first few EOFs of Spanish and Portuguese precipitation, and then in sec-

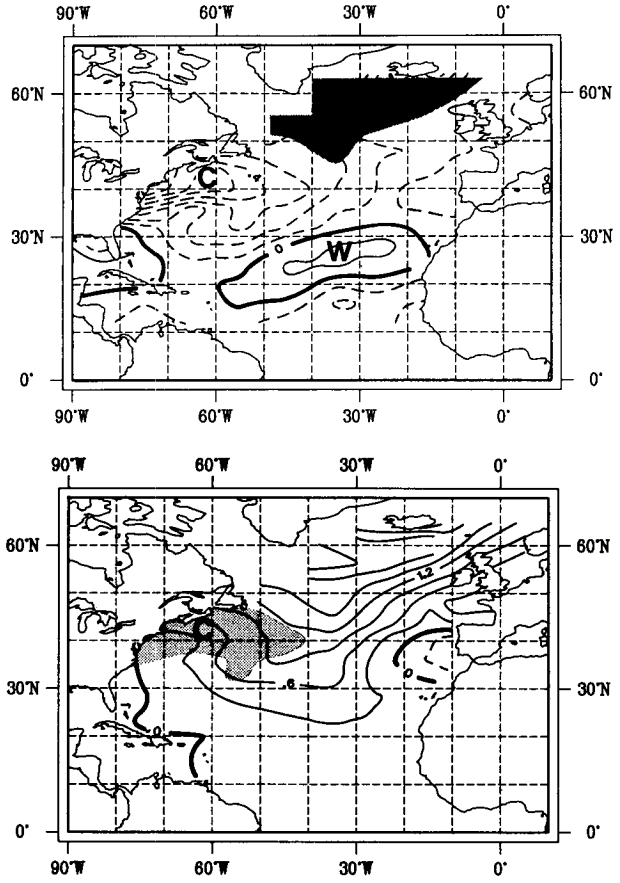

FIG. 8. The patterns of the first canonical pair of SST (K; contour interval 0.1 K) and σ_{SLP} (mb; contour interval 0.3 mb) in the North Atlantic area. The correlation between the corresponding time components is 0.52. They explain 12% and 14% of the total variance. In each figure, hatched areas correspond to maxima or minima in the other figure. Continuous lines mark positive values, and dashed lines negative values. The zero line is in bold.

tion 5b the canonical correlations between Atlantic SLP, SST, and the regional Iberian rainfall.

a. EOFs of Iberian rainfall

The first two eigenvalues of the covariance matrix explain 69% and 15% of the total DJF mean rainfall variance and stand out sufficiently clear from the background noise in terms of Rule N (Overland and Preisendorfer 1982).

The first EOF (Fig. 9a) shows the same sign over the entire area with higher values near the Atlantic coast and decreasing values toward the Mediterranean. The high percentage of variance explained by this pattern could be misleading, however. The distribution of stations is irregular, with a higher density in Portugal; if many stations cluster in a particular subarea, the amount of variance in this subregion is overrepresented in the total variance, and the eigenvalues associated with patterns that have the same sign over this subregion tend to be anomalously high. To check this problem, the rainfall EOFs have been also calculated including data from 42 additional Spanish stations (provided by Universidad Complutense, Madrid), and the results indicated in Fig. 9 were essentially confirmed. The uniform sign of the first pattern suggests that in spite of the highly irregular topography of the region studied there is a common physical process dominating the seasonal precipitation variability. Since this pattern reaches its highest values near the Atlantic coast, it is reasonable to assume that this pattern of variation is associated either with the strength of the mean westerly winds advecting precipitating synoptic systems to Iberia or with the sea surface temperature off the coast. We will return to this aspect in section 5b. The second EOF (Fig. 9b) has a dipole structure with positive and negative values being separated by a line connecting the southern end of Portugal and the Bay of Biscay. Possibly, this pattern could be linked to cyclonic activity that originated in the Mediterranean basin (Goosens 1985).

These results agree with those reported by Goosens (1985) in a study of precipitation patterns in the entire European–Mediterranean region.

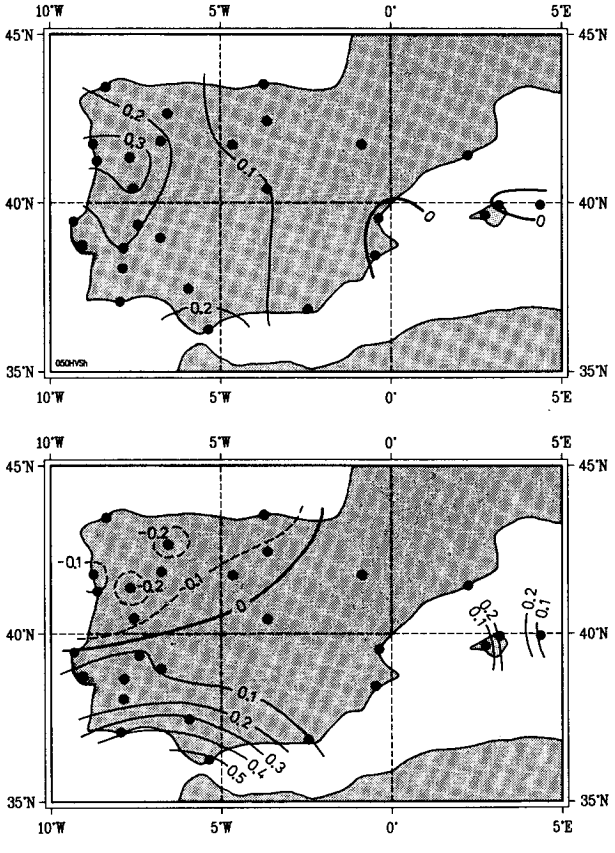

FIG. 9. First (a) and second (b) EOFs patterns of total winter (DJF) rainfall variability over the Iberian Peninsula. Dots mark the location of individual stations used in this study. The variances are $(583\ \text{mm})^2$ and $(255\ \text{mm})^2$, representing 68% and 13% of the total variance.

b. CCA of Iberian rainfall, mean SLP, and mean SST

The SLP pattern with the largest canonical correlation (.74) with Iberian winter precipitation accounts for 39% of the total seasonal mean SLP variance (Fig. 10a). It is essentially composed of the reversed first EOF shown in Fig. 2a. The CCA precipitation pattern explains 65% of the total rainfall variance, and the absolute value of its spatial coefficients are higher near the Atlantic coast, with values decreasing toward the east (Fig. 10b). Lower than normal sea level pressure over the northeastern Atlantic at midlatitudes and an anomalous anticyclonic circulation over the eastern Atlantic at high latitudes are described as being associated with higher precipitation over the Iberian Peninsula. From the physical point of view, these results seem very reasonable since low pressure in the mid-Atlantic guides maritime air and precipitating weather systems into Iberia.

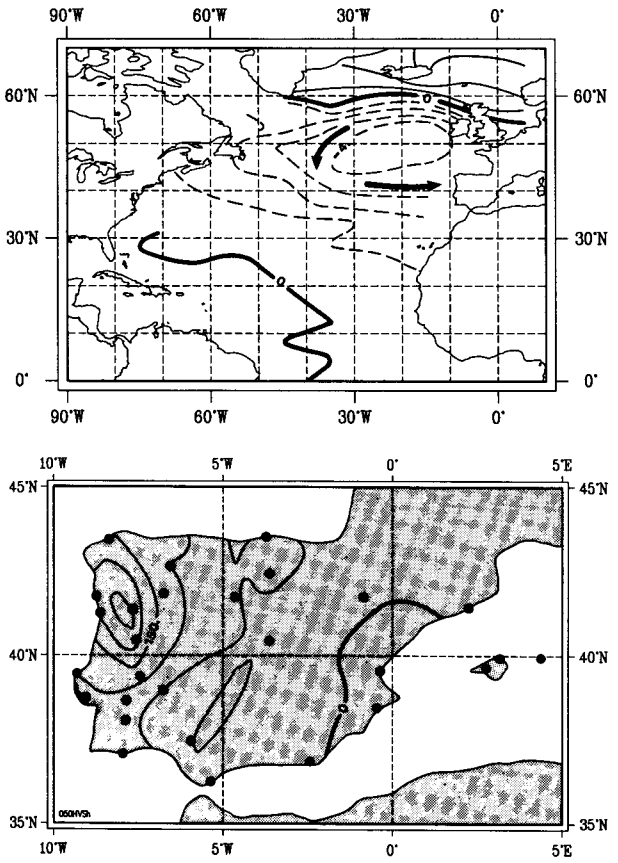

FIG. 10. The patterns of the first canonical pair of winter mean SLP (mb; contour interval 1 mb) in the North Atlantic and total winter (DJF) Iberian rainfall (mm; contour interval 50 mm). The correlation between the corresponding time components is 0.74. They explain 39% and 65% of the total variance. Continuous lines mark positive values, and dashed lines negative values. The zero line is in bold.

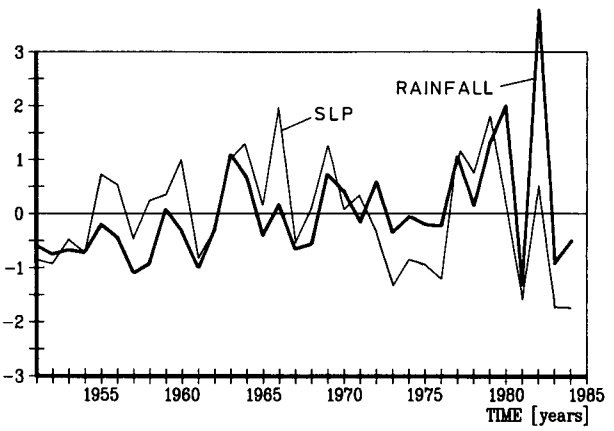

FIG. 11. Normalized time components of the CCA patterns of SLP anomalies and Iberian rainfall anomalies (Fig. 10).

In Fig. 11, the time coefficients of the CCA pair of mean SLP and Iberian rainfall are shown. It seems that the high correlation of .74 is not due to a few events but describes the similarity of the two curves throughout the entire 36-year record. The year-to-year variations are very coherent, but there are some discrepancies on a multiyear time scale. There is a weak trend in the rainfall data. After correction of this linear trend, the results remain essentially the same.

The CCA patterns (Fig. 12) of Atlantic SST and Iberian rainfall explain 13% and 65% of variance, respectively. The patterns appear inconsistent with the idea that more rainfall is associated with an increased reservoir of water vapor due to higher SST in most of the Atlantic west of the Iberian Peninsula. Another possible interpretation, namely that lower SST in the Atlantic at midlatitudes is responsible for the installation of a low offshore the Iberian Peninsula, is in conflict with the concepts presented in the Introduction (Fig. 1a). It seems then that the two patterns, in spite of their high canonical correlation (.70), are not causal to each other. Instead, the fact that the two patterns shown in Figs. 10a (SLP) and 12a (SST) are, once their sign is reversed, similar to the second SLP/SST CCA pair of patterns (Fig. 6) suggests that the SLP drives both the Iberian precipitation and Atlantic SST anomalies. Also, the rainfall pattern is almost the same as that identified in the SLP–rainfall CCA (Fig. 10b), and the SST pattern is very similar to the SST pattern in the second SLP–SST CCA (Fig. 6b). The plausible physical interpretation of the SLP–SST CCA (section 4b) is that the mean SLP forces the SST.

6. Discussion and conclusions

This study has focused on the wintertime atmosphere–ocean interactions on monthly time scales in the North Atlantic area, as well as their influence upon rainfall in the Iberian Peninsula. The major conclusions of the present study may be summarized as follows.

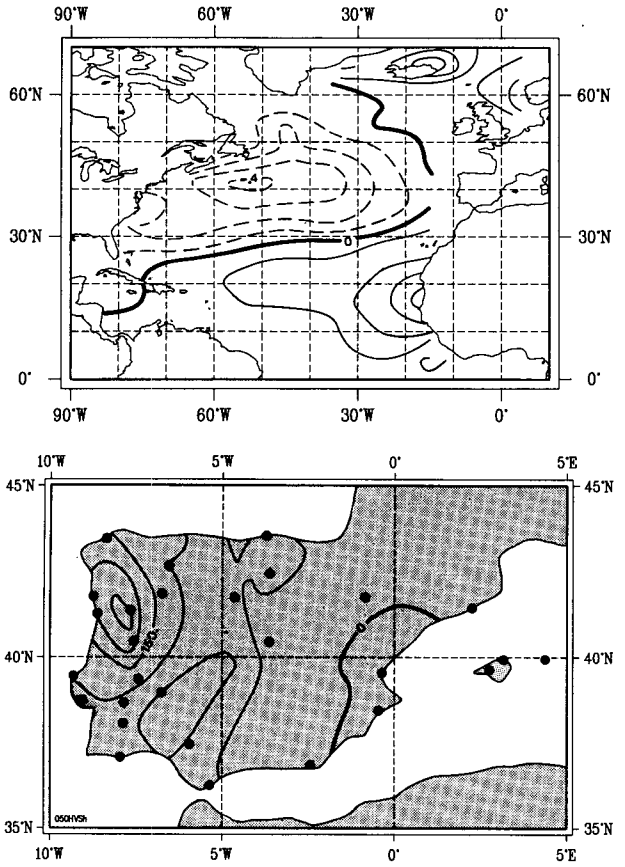

FIG. 12. The patterns of the first canonical pair of SST (K; contour interval 0.1 K) in the North Atlantic and of winter (DJF) Iberian rainfall (mm; contour interval 50 mm). The correlation between the corresponding time components is 0.70. They explain 13% and 65% of the total variance. Continuous lines mark positive values, and dashed lines negative values. The zero line is in bold.

1) *A great part of the North Atlantic SST variability can be explained as a result of atmospheric forcing.* The mechanisms of this forcing may be described in terms of simple notions concerning anomalous heat advection from adjacent areas or from the continent, increased heat fluxes due to intensified winds, and enhanced surface mixing by anomalous wind stress (Fig. 1b).

2) In accordance with the Barnett et al. (1984) analysis, *no indications were detected by our analysis that anomalous North Atlantic SST might exert a notable influence on the state of the overlying atmosphere.* In particular, an SST–SLP pattern configuration as predicted by the theory (Egger 1977; Webster 1981) was not found. Also, areas with warmer SST were not found to be associated with increased intramonthly variability as a result of reduced static stability of the atmosphere, locally or downstream of the anomalous SST. Instead, negative SST anomalies are connected with enhanced intramonthly activity, indicating that it is the SST responding to anomalous atmospheric forcing. Therefore, the possibility of SST anomalies being the origin of the observed large-scale SLP patterns in the North Atlantic is improbable.

3) *Anomalies of the spatial patterns of the atmospheric variability on intramonthly time scales,* as measured by σ_{SLP}, *occur simultaneously with large-scale anomalies of the monthly mean SLP.* Of course, these anomalies represent dynamically the two sides of the same coin.

4) *A large-scale SLP pattern, essentially the first EOF, is the most important atmospheric phenomenon in the Atlantic area associated with Iberian winter rainfall.* To check if the results reported by Lamb and Peppler (1987) concerning the influence of the NAO on Moroccan winter rainfall also apply to the Iberian rainfall, the correlations between the Sir Gilbert Walker's classical NAO index (Ponta Delgadas, Azores, minus Akureyri, Iceland, winter mean SLP) and the individual rainfall records (Fig. 13) have been calculated. At 15 of 29 stations the local correlation is significantly different from zero at the 90% level. According to the Livezey and Chen (1983) field test, the chance of observing that number of local rejections of the local null hypothesis is less than 0.1% if the two parameters were unrelated. It should be noted that the canonical correlation coefficient between the SLP field and Iberian rainfall (.74, section 5b) must be higher than every individual correlation shown in Fig. 13, since the canonical correlation coefficient is the highest attainable with linear combinations of station time series. If one station correlates better with any linear combination of the SLP field (in particular with the NAO index), then the trivial pattern formed with only this single station would be the canonical correlation pattern, and the canonical correlation coefficient would be precisely this higher correlation.

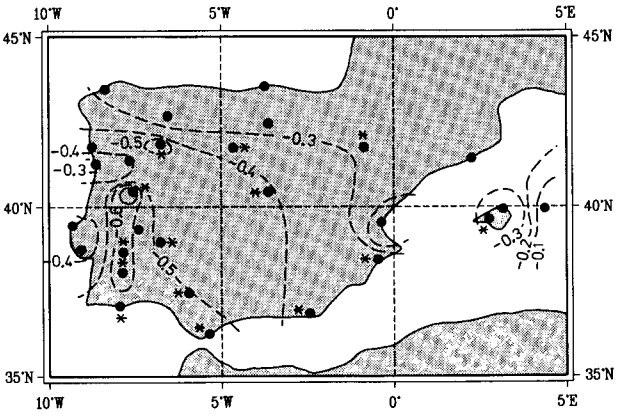

FIG. 13. The correlations between the North Atlantic Oscillation Index (Ponta Delgada, Azores, minus Akureyri, Iceland, winter mean SLP) and the winter precipitation record of each station in the Iberian Peninsula. The position of individual stations is marked by dots and stars. The latter refer to correlations that are significantly different from zero at the 90% level.

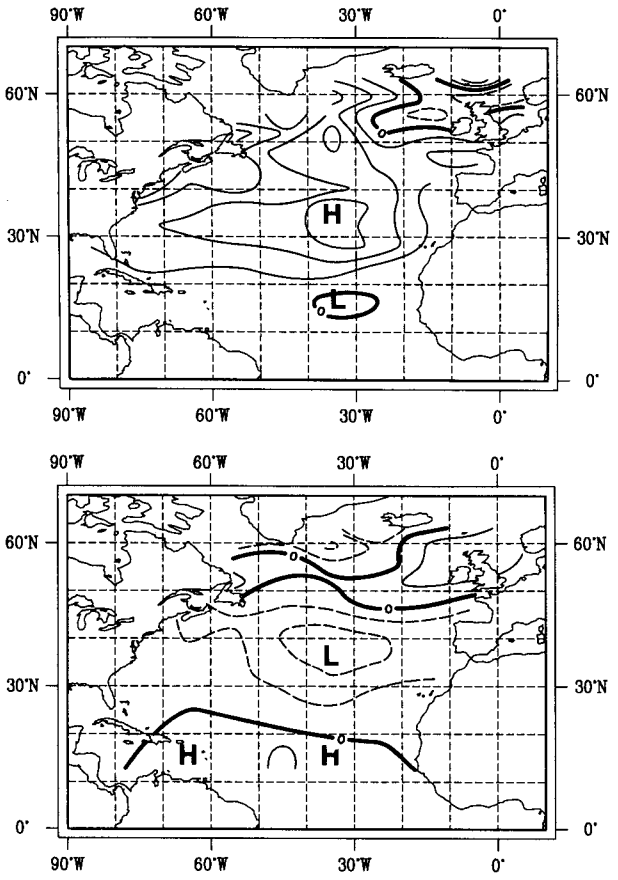

FIG. 14. Composite patterns of the σ_{SLP} (mb; contour 1 mb) field for (a) the ten most wet and (b) the ten most dry winters in the Iberian Peninsula.

5) *Large-scale North Atlantic SST anomalies, which appear at the same time as Iberian rainfall anomalies, are related to each other only indirectly.* Both are forced by the large-scale state of the atmosphere.

6) *The Iberian rainfall variability appears to be primarily determined by* the first SLP EOF, or equivalently, *by the intensity and number of storms in the central North Atlantic.* In Fig. 14, two composite patterns of the σ_{SLP} field in the North Atlantic for the ten most wet and ten most dry winters in the Iberian Peninsula are presented. The two patterns are almost mirror images of each other, with a dominating maximum–minimum in the central North Atlantic and a minor opposite extreme in the Great Britain area. Lau (1988) found that baroclinicity, measured by the bandpass-filtered σ_{SLP} (with periods of 2–6 days) in this region of the Atlantic is associated with the North Atlantic Oscillation. Clearly wet (dry) winters are associated with enhanced (reduced) baroclinic activity located upstream of the mean westerly flow in the central North Atlantic.

Acknowledgments. Compilation of COADS data at MPI in Hamburg was accomplished by Peter Wright. The data-retrieval software was developed by Ingo Jessel. Scott Woodruff supplied us with the updates of COADS. Ute Luksch, Rita Glowienka-Hense, Andreas Hense, and Hans Graf helped us with valuable comments. The diagrams were thoroughly prepared by Marion Grunert and Doris Lewandowski. We wish to thank all of them. Two of the authors received financial support from the Spanish Ministry of Science (E.Z.) and F.V.S. Foundation in Hamburg (Germany) (V.K.).

REFERENCES

Anderson, C. W., 1984: *An Introduction to Multivariate Statistical Analysis,* 2nd ed. Wiley & Sons, 675 pp.

Barnett, T., and R. Preisendorfer, 1987: Origins and levels of monthly and seasonal forecasts skill for United States surface air temperatures determined by canonical correlation analysis. *Mon. Wea. Rev.,* **115,** 1825–1850.

——, H. Heinz, and K. Hasselmann, 1984: Statistical predictions of seasonal air temperature over Eurasia. *Tellus,* **36A,** 132–146.

Barnston, G., and R. Livezey, 1987: Classification, seasonality, and persistence of low-frequency atmosphere circulation patterns. *Mon. Wea. Rev.,* **115,** 1083–1126.

Bjerknes, J., 1962: Synoptic survey of the interaction between sea and atmosphere in the North Atlantic. *Geofys. Publ.,* **24,** 116–145.

Cayan, D., 1990: Variability of latent and sensible heat fluxes over the oceans. Ph.D. dissertation, University of California, San Diego.

Davis, R., 1976: Predictability of sea surface temperature and sea surface pressure anomalies over the North Pacific Ocean. *J. Phys. Oceanogr.,* **6,** 249–266.

Dymnikov, V. P., and S. K. Filin, 1985a: A study of the correlations between sea surface anomalies in midlatitudes and anomalies in heating, based on data from the First GARP Global Experiment. Reprint of the Department of Numerical Mathematics of the USSR Academy of Sciences, N 84 (Moscow, USSR).

——, and ——, 1985b: Numerical simulations of the atmospheric response to sea surface temperature anomalies in the North Atlantic. Reprint of the Department of Numerical Mathematics of the USSR Academy of Sciences, N 83 (Moscow, USSR).

Egger, J., 1977: On the linear theory of the atmospheric response to sea surface temperature anomalies. *J. Atmos. Sci.,* **34,** 603–614.

Frankignoul, C., 1985: Sea surface temperature anomalies, planetary waves and air-sea feed back in the middle latitudes. *Rev. Geophys.,* **23,** 357–390.

——, and A. Molin, 1988: Response of the GISS general circulation model to a midlatitude sea surface temperature anomaly in the North Pacific. *J. Atmos. Sci.,* **45,** 95–108.

Glowienka-Hense, R., 1990: Performance of the ECMWF T21 model in simulating the North Atlantic Oscillation in the Atlantic–European SLP field. *Tellus,* **42A,** 497–507.

Goosens, C., 1985: Principal components analysis of Mediterranean rainfall. *J. Climatol.,* **5,** 379–388.

Hannoschöck, G., and C. Frankignoul, 1985: Multivariate statistical analysis of a sea surface temperature anomaly experiment with the GISS general circulation model 1. *J. Atmos. Sci.,* **42,** 1430–1450.

Hense, A., R. Glowienka-Hense, and H. von Storch, 1990: Northern Hemisphere atmospheric response to changes of Atlantic Ocean SST on decadal time scales: A GCM experiment. *Clim. Dyn.,* **4,** 157–174.

Hotelling, H., 1936: Relations between two sets of variates. *Biometrika,* **28,** 321–377.

Hunt, B., and H. Gordon, 1988: The problem of naturally occurring drought. *Clim. Dyn.,* **3,** 19–33.

Kalnay, E., K. Mo, and J. Peagle, 1986: Large amplitude, short-scale

stationary Rossby waves in the Southern Hemisphere: Observations and mechanistic experiments to determine their origin. *J. Atmos. Sci.*, **43**, 252–275.

Kutzbach, J., 1970: Large scale features of monthly mean Northern Hemisphere anomaly map of sea level pressure. *Mon. Wea. Rev.*, **98**, 708–716.

Lamb, P., and R. Peppler, 1987: The North Atlantic Oscillation: Concept and a Application. *Bull. Amer. Meteor. Soc.*, **68**, 1218–1225.

Lau, N.-C., 1988: Variability of the observed midlatitude storm tracks in relation to low-frequency changes in the circulation pattern. *J. Atmos. Sci.*, **45**, 2718–2743.

——, and M. J. Nath, 1990: A general circulation model study of the atmospheric response to extratropical SST anomalies observed in 1950–79. *J. Climate*, **3**, 713–725.

Livezey, R., and Y. Chen, 1983: Statistical field significance and its determination by Monte Carlo techniques. *Mon. Wea. Rev.*, **111**, 46–59.

Luksch, U., H. von Storch, and E. Maier-Reimer, 1990: Modeling North pacific SST anomalies as a response to anomalous atmospheric forcing. *J. Mar. Sys.*, **1**, 155–168.

Metz, W., 1989: Low-frequency anomalies of atmospheric flow and the effects of cyclone-scale eddies: A canonical correlation analysis. *J. Atmos. Sci.*, **46**, 1026–1041.

Mo, K., J. Pfaendtner, and E. Kalney, 1987: A GCM study of the maintenance of the June 1982 blocking in the Southern Hemisphere. *J. Atmos. Sci.*, **44**, 1123–1242.

Namias, J., 1978: Multiple causes of the North American abnormal winter. *Mon. Wea. Rev.*, **106**, 279–295.

——, and D. R. Cayan, 1982: Large-scale air–sea interactions and short-period climate fluctuations. *Science*, **214**, 869–876.

Overland, J., and R. Preisendorfer, 1982: A significance test for principal components applied to a cyclone climatology. *Mon. Wea. Rev.*, **110**, 1–4.

Palmer, T. N., and Z. Sun, 1985: A modelling and observational study of the relationship between sea surface temperature in northwest Atlantic and the atmospheric general circulation. *Quart. J. Roy. Meteor. Soc.*, **111**, 947–975.

Pitcher, E. J., M. L. Blackmon, G. Bates, and S. Muñoz, 1988: The effect of North Pacific sea surface temperature anomalies on the January climate of a general circulation model. *J. Atmos. Sci.*, **45**, 173–188.

Ratcliffe, R., and R. Murray, 1970: New lag associations between North Atlantic sea temperature and European pressure applied to long-range weather forecasting. *Quart. J. Roy. Meteor. Soc.*, **96**, 226–246.

Richman, M., 1986: Rotation of principal components. *J. Climatol.*, **6**, 293–335.

Rogers, J. C., 1984: The association between the North Atlantic oscillation and the Southern oscillation in the Northern Hemisphere. *Mon. Wea. Rev.*, **112**, 1999–2015.

——, and H. van Loon, 1979: The seesaw in winter temperature between Greenland and Northern Europe. Part II: Some oceanic and atmospheric effects in middle and high latitudes. *Mon. Wea. Rev.*, **107**, 509–519.

Rowntree, P., 1972: The influence of tropical east Pacific Ocean temperatures on the atmosphere. *Quart. J. Roy. Meteor. Soc.*, **98**, 290–321.

van Loon, H., and J. Rogers, 1978: The seesaw in winter temperature between Greenland and Northern Europe. Part I: General description. *Mon. Wea. Rev.*, **106**, 296–310.

Wallace, J. M., and Q. Jiang, 1987: On the observed structure of the interannual variability of the atmosphere–ocean climate system. *Atmospheric and Ocean Variability*, H. Cattle, Ed., Roy. Meteor. Soc., 17–43.

——, C. Smith, and Q. Jiang, 1990: Spatial patterns of atmospheric–ocean interaction in the northern winter. *J. Climate*, **3**, 990–998.

Weare, B. C., 1977: Empirical orthogonal analysis of Atlantic Ocean surface temperature. *Quart. J. Roy. Meteor. Soc.*, **103**, 467–478.

Webster, P., 1981: Mechanism determining the atmosphere response to sea surface temperature anomalies. *J. Atmos. Sci.*, **38**, 554–571.

Woodruff, S. D., R. J. Slutz, R. L. Jenne, and P. M. Steuer, 1987: A Comprehensive Ocean–Atmosphere Data Set. *Bull. Amer. Meteor. Soc.*, **68**, 1239–1250.